

Chapter 9

Finite and Infinite-Precision Properties of QRD-RLS Algorithms

Paulo S. R. Diniz and Marcio G. Siqueira

Abstract This chapter analyzes the finite and infinite-precision properties of QR-decomposition recursive least-squares (QRD-RLS) algorithms with emphasis on the conventional QRD-RLS and fast QRD-lattice (FQRD-lattice) formulations. The analysis encompasses deriving mean squared values of internal variables in steady-state and also the mean squared error of the deviations of the same variables assuming fixed-point arithmetic. In particular, analytical expressions for the excess of mean squared error and for the variance of the deviation in the tap coefficients of the QRD-RLS algorithm are derived, and the analysis is extended to the error signal of the FQRD-lattice algorithm. All the analytical results are confirmed to be accurate through computer simulations. Conclusions follow.

9.1 Introduction

The implementation of the QR-decomposition recursive least-squares (QRD-RLS) algorithm requires the knowledge of the dynamic range of its internal variables in order to determine their wordlengths. For the systolic array implementation of the QRD-RLS algorithm, the steady-state values of the cosines and sines of the Givens rotations and the bounds for the dynamic range of the processing cells contents are known [1]. An attractive feature of the QRD-RLS algorithm is the bounded input/bounded output stability, as proven in [1, 2].

In this chapter, we present a complete quantitative analysis of the dynamic range of all internal quantities of the QRD-RLS and fast QRD (FQRD)-lattice algorithms.

Paulo S. R. Diniz
Federal University of Rio de Janeiro (UFRJ), Rio de Janeiro – Brazil
e-mail: diniz@lps.ufrj.br

Marcio G. Siqueira
Cisco Systems, Inc., San Jose, CA – USA
e-mail: mgs@cisco.com

First, stability conditions for the QRD-RLS algorithm are derived by examining the quantization error propagation in all recursive equations of the algorithm assuming fixed-point arithmetic. In addition, the mean squared value of the errors accumulated in all variables of the algorithm are derived and accurate expressions for the excess of mean squared error and the mean squared value of the error in the filter coefficients are proposed for the conventional QRD-RLS algorithm. The results are later extended to the FQRD-lattice algorithm. Simulations follow finite-precision analysis. The chapter is concluded with a discussion on the derived and simulated results.

9.2 Precision Analysis of the QR-Decomposition RLS Algorithm

RLS algorithms update the adaptive filter coefficients in order to minimize the following objective (cost) function

$$\xi(k) = \sum_{i=0}^k \lambda^{k-i} |\bar{e}(i)|^2 = \sum_{i=0}^k [d(i) - \mathbf{w}^T(k)\mathbf{x}(i)]^2, \quad (9.1)$$

where $\mathbf{x}(k) = [x(k) \ x(k-1) \ \cdots \ x(k-N)]^T$ is the input signal vector, $\mathbf{w}(k) = [w_0(k) \ w_1(k) \ \cdots \ w_N(k)]^T$ is the coefficient vector at instant k , $\bar{e}(i)$ is the output error at instant i (computed with $\mathbf{w}(k)$), and λ is the forgetting factor. The input signal $x(k)$ is considered a Gaussian distributed white random variable with zero mean and variance σ_x^2 . However, the analysis is extended for non-white inputs.

The error vector, the reference signal vector, and the input signal information matrix can be defined, respectively, as

$$\mathbf{e}^T(k) \triangleq [\bar{e}(k) \ \lambda^{1/2}\bar{e}(k-1) \ \cdots \ \lambda^{k/2}\bar{e}(0)], \quad (9.2)$$

$$\mathbf{d}^T(k) \triangleq [d(k) \ \lambda^{1/2}d(k-1) \ \cdots \ \lambda^{k/2}d(0)], \text{ and} \quad (9.3)$$

$$\begin{aligned} \mathbf{X}^T(k) &\triangleq [\mathbf{x}(k) \ \lambda^{1/2}\mathbf{x}(k-1) \ \cdots \ \lambda^{k/2}\mathbf{x}(k)] \\ &= \begin{bmatrix} x(k) & \lambda^{1/2}x(k-1) & \cdots & \lambda^{k/2}x(0) \\ x(k-1) & \lambda^{1/2}x(k-2) & \cdots & 0 \\ \vdots & \vdots & \ddots & \vdots \\ x(k-N) & \lambda^{1/2}x(k-N-1) & \cdots & 0 \end{bmatrix}, \end{aligned} \quad (9.4)$$

so that the objective function can be rewritten as $\xi(k) = \mathbf{e}^T(k)\mathbf{e}(k)$, where $\mathbf{e}(k) = \mathbf{d}(k) - \mathbf{X}(k)\mathbf{w}(k)$.

The input data matrix $\mathbf{X}(k)$ can be triangularized through Givens rotations. The resulting triangularized matrix $\mathbf{U}(k)$, assuming the case of upper triangularization, may be given by

$$\mathbf{U}(k) \triangleq \begin{bmatrix} u_{0,0}(k) & u_{0,1}(k) & \cdots & u_{0,N}(k) \\ 0 & u_{1,1}(k) & \cdots & u_{1,N}(k) \\ \vdots & \vdots & \ddots & \vdots \\ 0 & 0 & \cdots & u_{N,N}(k) \end{bmatrix}. \quad (9.5)$$

When the orthogonal transformation denoted by $\mathbf{Q}(k)$ is applied to the error vector, it follows that:

$$\begin{aligned} \mathbf{Q}(k)\mathbf{e}(k) &= \mathbf{Q}(k)\mathbf{d}(k) - \mathbf{Q}(k)\mathbf{X}(k)\mathbf{w}(k) = \hat{\mathbf{d}}(k) - \hat{\mathbf{X}}(k)\mathbf{w}(k) \\ &= \begin{bmatrix} \hat{\mathbf{e}}_1(k) \\ \hat{\mathbf{e}}_2(k) \end{bmatrix} = \begin{bmatrix} \hat{\mathbf{d}}_1(k) \\ \hat{\mathbf{d}}_2(k) \end{bmatrix} - \begin{bmatrix} \mathbf{0}_{k-N,N+1} \\ \mathbf{U}(k) \end{bmatrix} \mathbf{w}(k). \end{aligned} \quad (9.6)$$

The QRD-RLS algorithm shown in Table 9.1 originates from the formulation above, see [3–5] for details. The operator $\mathbf{Q}[\cdot]$ denotes quantization and should be ignored in the discussions of the current section. The notation f_Q denotes finite-precision version of f .¹

In Equations (9.7) and (9.8), $a_{i,i}(k)$ (not explicitly shown) represents an intermediate quantity that appears in the position $(1, i)$ of the matrix $\mathbf{Q}'_{i-1}(k) \cdots \mathbf{Q}'_0(k)\mathbf{X}^p(k)$ (see (9.11)), that will be eliminated by the Givens rotation $\mathbf{Q}'_i(k)$. Quantities $b_i(k)$ represent intermediate values of the first element of $\mathbf{Q}'_{i-1}(k) \cdots \mathbf{Q}'_0(k)\mathbf{d}_2^p(k)$.

9.2.1 Infinite-precision analysis

Let's now derive the mean squared value of several quantities related to the QRD-RLS algorithm, namely $\cos \theta_i(k)$, $\sin \theta_i(k)$, $u_{i,j}(k)$, $a_{i,j}(k)$, $\hat{d}_{2,i}(k)$, $b_i(k)$, and $e_q(k)$. These results are required to analyze the QRD algorithm implemented with finite precision.

It is worth mentioning that the analysis is valid for averages taken as k is large. Although the label k is redundant in most expressions it can be useful for transient analysis.

9.2.1.1 Mean squared values of sines and cosines

From the implementation of (9.7), (9.8), (9.10), and (9.11), with infinite-precision arithmetic, it is can be shown that

$$u_{i,i}(k) = \sqrt{\lambda u_{i,i}^2(k-1) + a_{i,i}^2(k)}; \quad (9.18)$$

therefore,

¹ In practice, vectors and matrices with growing dimensions in Equations (9.7), (9.8), (9.9), (9.10), (9.11), (9.12), (9.13), (9.14), (9.15), (9.16), and (9.17) should be replaced by fixed dimension ones. This notation was chosen to clarify the presentation.

Table 9.1 Conventional QR-decomposition RLS algorithm.**QRD-RLS**

Matrix Formulation: For $i = 0, \dots, N$, do

$$\cos_Q \theta_i(k) = Q \left[z \frac{\lambda^{1/2} u_{i,i;Q}(k-1)}{Q \left[\sqrt{Q[\lambda u_{i,i;Q}^2(k-1) + a_{i,i;Q}^2(k)]} \right]} \right] \quad (9.7)$$

$$\sin_Q \theta_i(k) = Q \left[\frac{a_{i,i;Q}(k)}{Q \left[\sqrt{Q[\lambda u_{i,i;Q}^2(k-1) + a_{i,i;Q}^2(k)]} \right]} \right] \quad (9.8)$$

$$\mathbf{Q}'_{i;Q}(k) = \begin{bmatrix} \cos_Q \theta_i(k) & & -\sin_Q \theta_i(k) & & \\ & \mathbf{I}_{k-N+i-1} & & & \\ \sin_Q \theta_i(k) & & \cos_Q \theta_i(k) & & \\ & & & & \mathbf{I}_{N-i} \end{bmatrix} \quad (9.9)$$

$$\mathbf{X}_Q^p(k) = \begin{bmatrix} \mathbf{x}^T(k) \\ \mathbf{0}_{k-N-1, N+1} \\ \lambda^{1/2} \mathbf{U}_Q(k-1) \end{bmatrix} \quad (9.10)$$

$$\begin{aligned} \hat{\mathbf{X}}_Q(k) &= Q[\mathbf{Q}'_{N;Q}(k)Q[\mathbf{Q}'_{N-1;Q}(k) \cdots Q[\mathbf{Q}'_{0;Q}(k)\mathbf{X}_Q^p(k)] \cdots]] \\ &= Q[\hat{\mathbf{Q}}_Q(k)\mathbf{X}_Q^p(k)] \\ &= \begin{bmatrix} \mathbf{0}_{k-N, N+1} \\ \mathbf{U}_Q(k) \end{bmatrix} \end{aligned} \quad (9.11)$$

$$\mathbf{d}_Q^p(k) = \begin{bmatrix} d^*(k) \\ \lambda^{1/2} \hat{\mathbf{d}}_{1;Q}(k-1) \\ \lambda^{1/2} \hat{\mathbf{d}}_{2;Q}(k-1) \end{bmatrix} \quad (9.12)$$

$$\begin{aligned} \hat{\mathbf{d}}_Q(k) &= Q[\mathbf{Q}'_{N;Q}(k)Q[\mathbf{Q}'_{N-1;Q}(k) \cdots Q[\mathbf{Q}'_{0;Q}(k)\mathbf{d}_Q^p(k)] \cdots]] \\ &= Q[\hat{\mathbf{Q}}_Q(k)\mathbf{d}_Q^p(k)] \\ &= \begin{bmatrix} e_{q;Q}(k) \\ \hat{\mathbf{d}}_{1;Q}(k) \\ \hat{\mathbf{d}}_{2;Q}(k) \end{bmatrix} \end{aligned} \quad (9.13)$$

Back-substitution: For $j = 0, \dots, N$ do

$$f_{j;Q}(k) = Q \left[\sum_{i=j+1}^N w_{i;Q}(k) u_{j,i;Q}(k) \right] \quad (9.14)$$

$$w_{j;Q}(k) = Q \left[\frac{d_{2,j;Q}(k) - f_{j;Q}(k)}{u_{j,j;Q}(k)} \right] \quad (9.15)$$

Error calculation: Use one of the equations

$$e_Q(k) = Q[e_{q;Q}(k)Q[\cos_Q \theta_0(k) \cdots Q[\cos_Q \theta_N(k) \cos_Q \theta_{N-1}(k)] \cdots]] \quad (9.16)$$

$$e_Q(k) = d(k) - Q[\mathbf{w}_Q^T(k)\mathbf{x}(k)] \quad (9.17)$$

$$\cos \theta_i(k) = \frac{\lambda^{1/2} u_{i,i}(k-1)}{u_{i,i}(k)}, \text{ and} \quad (9.19)$$

$$\sin \theta_i(k) = \frac{a_{i,i}(k)}{u_{i,i}(k)}. \quad (9.20)$$

The mean squared value of $\cos \theta_i(k)$ is then given by

$$E \{ \cos^2 \theta_i(k) \} = E \left\{ \lambda \frac{\sum_{j=0}^{k-1} \lambda^{k-1-j} a_{i,i}^2(j)}{\sum_{j=0}^k \lambda^{k-j} a_{i,i}^2(j)} \right\} \approx \lambda. \quad (9.21)$$

whereas the mean squared value of $\sin \theta_i(k)$ can be calculated by using the fundamental trigonometric identity

$$E \{ \sin^2 \theta_i(k) \} \approx 1 - \lambda, \quad (9.22)$$

for $k \rightarrow \infty$.

9.2.1.2 Mean squared value of $u_{i,j}(k)$

The derivations of the mean squared values of the elements of $\mathbf{U}(k)$ are somewhat involved, especially when the order of the adaptive filter is high. Under the assumption that the input signal samples are uncorrelated, it is possible to deduce the desired formulas [6]:

$$E \{ u_{i,i}^2(k) \} \approx \frac{\sigma_x^2}{1-\lambda} \left[\frac{2\lambda}{1+\lambda} \right]^i, \text{ and} \quad (9.23)$$

$$E \{ u_{i,j}^2(k) \} \approx \frac{\sigma_x^2}{1+\lambda} \left[\frac{2\lambda}{1+\lambda} \right]^i, \quad (9.24)$$

where the last equation is valid for $j > i$, $i = 0, 1, \dots, N$.

9.2.1.3 Mean squared value of $a_{i,j}(k)$

From (9.18), it is possible to verify that

$$E [u_{i,i}^2(k)] = \frac{E [a_{i,i}^2(k)]}{1-\lambda}. \quad (9.25)$$

From (9.25) and (9.23), one can show that

$$E \{ a_{i,i}^2(k) \} = \sigma_x^2 \left[\frac{2\lambda}{1+\lambda} \right]^i, \quad (9.26)$$

for $i = 0, \dots, N$. Since $a_{i,j}(k)$ for $i \neq j$ and $a_{i,i}(k)$ are result of similar dynamic equations, it is possible to show that

$$E\{a_{i,j}^2(k)\} = \sigma_x^2 \left[\frac{2\lambda}{1+\lambda} \right]^i, \quad (9.27)$$

for $i = 0, \dots, N$ and $j > i$.

9.2.1.4 Mean squared value of $\hat{\mathbf{d}}_{2,i}(k)$

The adaptive filter coefficients are calculated using (9.6), that is

$$\hat{d}_{2,i}(k) = \sum_{j=i}^N u_{i,j}(k) w_j(k). \quad (9.28)$$

If $u_{i,i}(k)$ is considered the only element in the i th row of $\mathbf{U}(k)$ with non-zero mean, and that the elements in a given row are uncorrelated, the following expression approximation is valid.

$$E\{\hat{d}_{2,i}^2(k)\} \approx \sum_{j=i}^N E\{u_{i,j}^2(k)\} E\{w_j^2(k)\} \quad (9.29)$$

In addition, considering that the mean of $w_i(k)$ is much larger than the variance, so that the mean squared value can be replaced by the squared mean, the equation becomes

$$E\{\hat{d}_{2,i}^2(k)\} \approx \left[\frac{2\lambda}{1+\lambda} \right]^i \left[\frac{\sigma_x^2}{1-\lambda} w_{o,i}^2 + \frac{\sigma_x^2}{1+\lambda} \sum_{j=i+1}^N w_{o,j}^2 \right], \quad (9.30)$$

where

$$w_{o,i}^2 = E\{w_i^2(k)\}. \quad (9.31)$$

9.2.1.5 Mean squared value of $b_i(k)$

The intermediate values of the first element of $\hat{\mathbf{d}}(k)$ during the application of the Givens rotations, denoted by $b_i(k)$ for $i = 0, 1, \dots, N$, are given by

$$b_{i+1}(k) = -\lambda^{1/2} \hat{d}_{2,i}(k-1) \sin \theta_i(k) + b_i(k) \cos \theta_i(k). \quad (9.32)$$

Since $E\{\cos \theta_i(k) \sin \theta_i(k)\}$ is relatively small, it is possible to infer that

$$\begin{aligned} E\{b_{i+1}^2(k)\} &= \lambda E\{\hat{d}_{2,i}^2(k-1)\} E\{\sin^2 \theta_i(k)\} + E\{b_i^2(k)\} E\{\cos^2 \theta_i(k)\} \\ &= \lambda(1-\lambda) E\{\hat{d}_{2,i}^2(k-1)\} + \lambda E\{b_i^2(k)\} \\ &= \sum_{j=1}^{i+1} \lambda^{i-j+2} (1-\lambda) E\{\hat{d}_{2,j}^2(k)\} + \lambda^{i+1} E\{d^2(k)\}. \end{aligned} \quad (9.33)$$

9.2.1.6 Mean squared value of $e_q(k)$

From (9.21) and (9.16), and by assuming that the mean values of the cosines are much larger than their variance [7], it is possible to verify that

$$E\{e_q^2(k)\} \approx \frac{E\{e^2(k)\}}{\lambda^{N+1}}. \quad (9.34)$$

If the QRD-RLS algorithm is applied in a sufficient order identification problem, where the desired signal can be modeled by a moving average process with a measurement noise with variance σ_r^2 . After convergence, it is expected that

$$E\{e_q^2(k)\} \approx \frac{\sigma_r^2}{\lambda^{N+1}}. \quad (9.35)$$

9.2.1.7 Dynamic range

The internal variables of the QRD-RLS algorithm are the elements of $\mathbf{U}(k)$, of $\hat{\mathbf{d}}_2(k)$, and the sines and cosines. Let's assume that all variables are represented in fixed-point arithmetic in the range -1 to $+1$, in order to derive the conditions on the input signal variance to ensure that overflow does not occur frequently in internal variables of the algorithm.

The off-diagonal elements of $\mathbf{U}(k)$ have zero mean and mean squared values much smaller than the diagonal elements. The diagonal elements usually have larger mean squared values as λ approaches 1; as such, some strategy to control the overflow must be devised. Considering that for λ close to one, the mean of $u_{i,i}(k)$ is large as compared to its standard deviation, one can calculate its mean squared value through its squared mean. From (9.23), it follows that

$$E\{u_{i,i}(k)\} \approx \frac{\sigma_x}{\sqrt{1-\lambda}} \left[\frac{2\lambda}{1+\lambda} \right]^{i/2}. \quad (9.36)$$

As $u_{0,0}(k)$ has the largest energy, and if the maximum value for $u_{0,0}(k)$ is 1, satisfying the condition

$$\frac{\sigma_x}{\sqrt{1-\lambda}} < 1 \quad (9.37)$$

is sufficient to avoid frequent internal overflow.

The values of the entries of $\hat{\mathbf{d}}_2(k)$ should also be kept in the range -1 and $+1$. For any k ,

$$E\{\hat{d}_{2,i}(k)\} = \sum_{j=i}^N E\{u_{i,j}(k)w_j(k)\}. \quad (9.38)$$

Assuming that the mean of $u_{i,j}(k)$ is zero for $i \neq j$, and that the standard deviations of $u_{i,i}(k)$ and $w_i(k)$ are small compared to their respective mean, it is possible to

verify that

$$\begin{aligned} E\{\hat{d}_{2,i}(k)\} &= E\{u_{i,i}(k)w_i(k)\} \approx E\{u_{i,i}(k)\}E\{w_i(k)\} \\ &= \frac{\sigma_x}{\sqrt{1-\lambda}} \left[\frac{2\lambda}{1+\lambda} \right]^{i/2} w_{o,i}. \end{aligned} \quad (9.39)$$

The most stringent case is $i = 0$, so that frequent overflows can be avoided if, the following inequality is satisfied:

$$\sigma_x^2 w_{o,i}^2 < 1 - \lambda. \quad (9.40)$$

This inequality requires the mean squared value of the taps $w_{o,i}$, that accounts for the relative power of the reference signal. Although the values of $w_{o,i}$ are not known in advance, a rough estimate of $\sigma_x^2 w_{o,i}^2$ can be obtained through the power of the reference signal [8].

9.2.2 Stability analysis

In this section, the fixed-point quantization errors are first modeled, and the recursive equations describing the total error in each quantity of the QRD-RLS algorithm are derived. For that, we discuss the conditions to guarantee the stability of the algorithm.

For the analysis results presented here, we assume that the input signal has been properly scaled in order to avoid overflow. Two's complement arithmetic is used for numeric representation. It is taken for granted that no overflow occurs so that additions and subtractions do not introduce quantization errors.

The multiplication, division, and square-root operations introduce, respectively, quantization errors described by

$$\eta_M(a, b) \triangleq ab - Q[ab], \quad (9.41)$$

$$\eta_D(a, b) \triangleq a/b - Q[a/b], \quad (9.42)$$

$$\eta_S(a) \triangleq \sqrt{a} - Q[\sqrt{a}], \quad (9.43)$$

where a and b are scalars. For inner product with quantization after addition, the errors are denoted as

$$\eta_M[(a_1, b_1); \dots; (a_i, b_i)] \triangleq \sum_{j=1}^i a_j b_j - Q \left[\sum_{j=1}^i a_j b_j \right]. \quad (9.44)$$

The quantization errors for matrix–vector and matrix–matrix products are modeled as

$$\eta_M(\mathbf{A}, \mathbf{b}) \triangleq \mathbf{A}\mathbf{b} - \mathbf{Q}[\mathbf{A}\mathbf{b}] \quad (9.45)$$

and

$$\mathbf{N}_M(\mathbf{A}, \mathbf{B}) \triangleq \mathbf{A}\mathbf{B} - \mathbf{Q}[\mathbf{A}\mathbf{B}], \quad (9.46)$$

respectively.

Instantaneous quantizations are performed by rounding, for any type of arithmetic. The quantization error has zero mean and variance $2^{-2B}/12$, where B is the number of bits excluding the sign.

The overall quantization error in each quantity is defined as the difference between its value in infinite-precision implementation and its value in finite-precision implementation, that is

$$\Delta a(k) \triangleq a(k) - a_Q(k). \quad (9.47)$$

Matrix $\hat{\mathbf{X}}(k)$ is defined as

$$\begin{aligned} \hat{\mathbf{X}}(k) &= \tilde{\mathbf{Q}}(k)\mathbf{X}^p(k) = [\tilde{\mathbf{Q}}_Q(k) + \Delta\tilde{\mathbf{Q}}(k)][\mathbf{X}_Q^p(k) + \Delta\mathbf{X}^p(k)] \\ &= \tilde{\mathbf{Q}}_Q(k)\mathbf{X}_Q^p(k) + \tilde{\mathbf{Q}}_Q(k)\Delta\mathbf{X}^p(k) + \Delta\tilde{\mathbf{Q}}(k)\mathbf{X}_Q^p(k) \\ &\quad + \Delta\tilde{\mathbf{Q}}(k)\Delta\mathbf{X}^p(k). \end{aligned} \quad (9.48)$$

From (9.11) and (9.47), it follows that

$$\begin{aligned} \tilde{\mathbf{Q}}_Q(k)\mathbf{X}_Q^p(k) &= \mathbf{Q}[\tilde{\mathbf{Q}}_Q(k)\mathbf{X}_Q^p(k)] + \mathbf{N}_M[\tilde{\mathbf{Q}}_Q(k), \mathbf{X}_Q^p(k)] \\ &= \hat{\mathbf{X}}(k) + \mathbf{N}_M[\tilde{\mathbf{Q}}_Q(k), \mathbf{X}_Q^p(k)]. \end{aligned} \quad (9.49)$$

It can then be shown that

$$\begin{aligned} \Delta\hat{\mathbf{X}}(k) &= \hat{\mathbf{X}}(k) - \hat{\mathbf{X}}_Q(k) = \tilde{\mathbf{Q}}_Q(k)\Delta\mathbf{X}^p(k) + \Delta\tilde{\mathbf{Q}}(k)\Delta\mathbf{X}^p(k) \\ &\quad + \Delta\tilde{\mathbf{Q}}(k)\mathbf{X}_Q^p(k) + \mathbf{N}_M[\tilde{\mathbf{Q}}_Q(k), \mathbf{X}_Q^p(k)]. \end{aligned} \quad (9.50)$$

Using (9.50), (9.10), the definition of (9.47) and considering that $\mathbf{U}(k) = \mathbf{U}_Q(k) + \Delta\mathbf{U}(k)$, we find that

$$\begin{aligned} \begin{bmatrix} \mathbf{0}_{k-N, N+1} \\ \Delta\mathbf{U}(k) \end{bmatrix} &= \tilde{\mathbf{Q}}_Q(k) \begin{bmatrix} \mathbf{0}_{k-N, N+1} \\ \lambda^{1/2}\Delta\mathbf{U}(k-1) \end{bmatrix} \\ &\quad + \Delta\tilde{\mathbf{Q}}(k) \begin{bmatrix} \mathbf{x}^T(k) \\ \mathbf{0}_{k-N-1, N+1} \\ \lambda^{1/2}\mathbf{U}(k-1) \end{bmatrix} + \mathbf{N}_M[\tilde{\mathbf{Q}}_Q(k), \mathbf{X}_Q^p(k)]. \end{aligned} \quad (9.51)$$

The above equation represents the dynamics of the error in the input signal matrix after triangularization. The convergence in average of $\mathbf{U}(k)$ can be guaranteed if the following inequality is satisfied

$$\lambda^{1/2} \|\tilde{\mathbf{Q}}_Q(k)\|_2 \leq 1, \quad (9.52)$$

where the two norm of a matrix is defined here as the square root of the largest eigenvalue. Hence,

$$\|\tilde{\mathbf{Q}}_Q(k)\|_2 = \text{MAX}_i \sqrt{\cos^2 \theta_i(k) + \sin^2 \theta_i(k)}. \quad (9.53)$$

Then, the stability condition can be rewritten as follows:

$$\lambda < \frac{1}{\text{MAX}_i [\cos^2 \theta_i(k) + \sin^2 \theta_i(k)]}. \quad (9.54)$$

By assuming instantaneous errors term non-zero in (9.51), we can show that

$$\begin{aligned} \|E\{\Delta \mathbf{U}(k)\}\| &\leq \lambda^{1/2} \|E\{\tilde{\mathbf{Q}}_Q(k)\}\| \|E\{\Delta \mathbf{U}(k-1)\}\| \\ &+ \|E\{\Delta \tilde{\mathbf{Q}}_Q(k)\}\| \|E\{\mathbf{X}(k)\}\|. \end{aligned} \quad (9.55)$$

Notice that (9.54) is also sufficient to guarantee that (9.55) is stable. For $\lambda = 1$ and $E\{\|\tilde{\mathbf{Q}}_Q(k)\|\} = 1$, the norm of $E[\Delta \mathbf{U}(k)]$ increases indefinitely, if the input signal is non-zero.

9.2.3 Error propagation analysis in steady-state

In this subsection, we derive the error propagation. Analytical expressions for the mean squared value of the errors in the prediction error and in the tap coefficients are obtained.

9.2.3.1 Mean squared value of $\Delta a_{i,j}(k)$

During the triangularization process, the intermediate value that the j th element of the first row of $\mathbf{X}^P(k)$ assumes in the i th Givens rotation is denoted as $a_{i,j}(k)$. These quantities are given by

$$a_{i+1,j}(k) = a_{i,j}(k) \cos \theta_i(k) - \lambda^{1/2} u_{i,j}(k-1) \sin \theta_i(k), \quad (9.56)$$

where $a_{0,j}(k) \triangleq x(k-j)$. The equation above can be solved recursively as

$$\begin{aligned}
 a_{i,j}(k) &= x(k-j) \prod_{m=0}^{i-1} [\cos_Q \theta_m(k) + \Delta \cos \theta_m(k)] \\
 &\quad - \lambda^{1/2} \sum_{m=0}^{i-1} [u_{m,j;Q}(k-1) + \Delta u_{i,j}(k-1)] [\sin_Q \theta_m(k) + \Delta \sin \theta_m(k)] \cdot \\
 &\quad \prod_{n=m+1}^{i-1} [\cos_Q \theta_n(k) + \Delta \cos \theta_n(k)], \tag{9.57}
 \end{aligned}$$

Note that in the last equality $a_{i,j}(k)$ is expressed as a function of the quantities in the finite-precision implementation and their respective errors. By neglecting all second-order and higher-order error terms, it follows that

$$\begin{aligned}
 a_{i,j}(k) &\approx x(k-j) \prod_{m=0}^{i-1} \cos_Q \theta_m(k) \\
 &\quad - \lambda^{1/2} \sum_{m=0}^{i-1} u_{m,j;Q}(k-1) \sin_Q \theta_m(k) \prod_{n=m+1}^{i-1} \cos_Q \theta_n(k) \\
 &\quad + x(k-j) \sum_{n=0}^{i-1} \Delta \cos \theta_n(k) \prod_{\substack{m=0 \\ m \neq n}}^{i-1} \cos_Q \theta_m(k) \\
 &\quad - \lambda^{1/2} \sum_{m=0}^{i-1} [u_{m,j;Q}(k-1) \Delta \sin \theta_m(k) \\
 &\quad + \Delta u_{m,j}(k-1) \sin_Q \theta_m(k)] \prod_{n=m+1}^{i-1} \cos_Q \theta_n(k) \\
 &\quad - \lambda^{1/2} \sum_{m=0}^{i-1} u_{m,j;Q}(k-1) \sin_Q \theta_m(k) \cdot \\
 &\quad \left\{ \sum_{n=m+1}^{i-1} \Delta \cos \theta_n(k) \prod_{\substack{q=0 \\ q \neq n}}^{i-1} \cos_Q \theta_q(k) \right\}. \tag{9.58}
 \end{aligned}$$

In finite-precision case, $a_{i,j;Q}(k)$ is given by

$$\begin{aligned}
 a_{i,j;Q}(k) &= x(k-j) \prod_{m=0}^{i-1} \cos_Q \theta_m(k) \\
 &\quad - \lambda^{1/2} \sum_{m=0}^{i-1} u_{m,j;Q}(k-1) \sin_Q \theta_m(k) \prod_{n=m+1}^{i-1} \cos_Q \theta_n(k) \\
 &\quad - \sum_{m=0}^{i-1} \eta_M^{aij}(k) \prod_{n=m+1}^{i-1} \cos_Q \theta_n(k), \tag{9.59}
 \end{aligned}$$

The quantities $\eta_M^{aij}(k) = \eta_M[(a_{i,j}(k), \cos \theta_i(k)); (\lambda^{1/2}u_{i,j}(k-1), \sin \theta_i(k))]$, for $m = 0, \dots, i$, represent quantization noises generated by the products.

From (9.57) and (9.59), it follows that

$$\begin{aligned} \Delta a_{i,j}(k) &= x(k-j) \sum_{n=0}^{i-1} \Delta \cos_Q \theta_n(k) \prod_{\substack{m=0 \\ m \neq n}}^{i-1} \cos_Q \theta_m(k) \\ &\quad - \lambda^{1/2} \sum_{m=0}^{i-1} [u_{m,j;Q}(k-1) \Delta \sin \theta_m(k) + \Delta u_{m,j}(k-1) \sin_Q \theta_m(k)] \cdot \\ &\quad \prod_{n=m+1}^{i-1} \cos_Q \theta_n(k) \lambda^{1/2} \sum_{m=0}^{i-1} u_{m,j;Q}(k-1) \sin_Q \theta_m(k) \cdot \\ &\quad \left\{ \sum_{n=m+1}^{i-1} \Delta \cos \theta_n(k) \prod_{\substack{q=m+1 \\ n \neq q}}^{i-1} \cos_Q \theta_q(k) \right\} \\ &\quad + \sum_{m=0}^{i-1} \eta_m^{aij}(k) \prod_{n=m+1}^{i-1} \cos_Q \theta_n(k). \end{aligned} \tag{9.60}$$

We assume now that $x(k)$, $\Delta \cos \theta_i(k)$, $\Delta \sin \theta_i(k)$, and $\eta_i^{aij}(k)$ are all zero mean with comparatively small cross-correlations. We also assume that $E\{u_{i,j;Q}^2(k-1)\}$ and $E\{[\Delta u_{i,j}(k-1)]^2\}$ can be replaced by $E\{u_{i,j;Q}^2(k)\}$ and $E\{[\Delta u_{i,j}(k)]^2\}$, respectively, by considering them stationary. Another assumption is that the mean squared value of quantities in finite and infinite-precision coincide. Therefore, using the assumptions (9.22) and (9.21), the resulting expression for the mean squared value of $\Delta a_{i,j}(k)$ is given by

$$\begin{aligned} E\{[\Delta a_{i,j}(k)]^2\} &= \sigma_x^2 \lambda^{i-1} \sum_{n=0}^{i-1} E\{[\Delta \cos \theta_n(k)]^2\} \\ &\quad + \sum_{m=0}^{i-1} \lambda^{i-m} \{E\{u_{m,j}^2(k)\}E\{[\Delta \sin \theta_m(k)]^2\} + E\{[\Delta u_{m,j}(k)]^2\}(1-\lambda)\} \\ &\quad + \sum_{m=0}^{i-1} \left\{ E\{u_{m,j}^2(k)\}(1-\lambda) \sum_{n=m+1}^{i-1} E\{[\Delta \cos \theta_n(k)]^2\} \lambda^{i-m-1} \right\} \\ &\quad + \frac{\lambda^i - 1}{\lambda - 1} \sigma_n^2, \end{aligned} \tag{9.61}$$

where σ_n^2 is the variance of $\eta_M^{aij}(k)$.

9.2.3.2 Mean squared value of $\Delta b_i(k)$

The values $b_i(k)$ correspond to the first element of the intermediate vectors resulting from the application of Givens rotations to vector $\hat{\mathbf{d}}_2(k)$. The form of deriving $\Delta b_i(k)$ is similar to $\Delta a_{i,j}(k)$ and the result is

$$\begin{aligned} \Delta b_i(k) &\approx d(k) \sum_{m=0}^{i-1} \Delta \cos \theta_m(k) \prod_{\substack{j=0 \\ j \neq m}}^{i-1} \cos \theta_j(k) \\ &\quad - \lambda^{1/2} \sum_{j=0}^{i-1} [\hat{d}_{2,j;Q}(k-1) \Delta \sin \theta_j(k) + \Delta \hat{d}_{2,j}(k-1) \sin \theta_j(k)] \cdot \\ &\quad \prod_{m=j+1}^{i-1} \cos_Q \theta_m(k) - \lambda^{1/2} \sum_{j=0}^{i-1} \hat{d}_{2,j;Q}(k-1) \sin_Q \theta_j(k) \cdot \\ &\quad \left\{ \sum_{p=j+1}^{i-1} \Delta \cos \theta_p(k) \prod_{\substack{m=j+1 \\ m \neq p}}^{i-1} \cos_Q \theta_m(k) \right\} \\ &\quad + \sum_{j=0}^{i-1} \eta_j^{bi}(k) \prod_{m=j+1}^{i-1} \cos_Q \theta_m(k), \end{aligned} \quad (9.62)$$

where $\eta_j^{bi}(k) = \eta_M[(b_{i-1}(k), \cos \theta_{i-1}(k)); (\lambda^{1/2} \hat{d}_{2,i-1}(k-1), \sin \theta_{i-1}(k))]$. Using the assumption that $\Delta \cos \theta_i(k)$, $\Delta \sin \theta_i(k)$, and $\eta_j^{bi}(k)$ are all zero mean and have small cross-correlation with each other and also assuming that $E\{\hat{d}_{2,j;Q}^2(k-1)\} = E\{\hat{d}_{2,j;Q}^2(k)\}$ and $E\{[\Delta \hat{d}_{2,j;Q}(k-1)]^2\} = E\{[\Delta \hat{d}_{2,j;Q}(k)]^2\}$, it can be shown that

$$\begin{aligned} E\{[\Delta b_i(k)]^2\} &= \sigma_x^2 \|\mathbf{w}_o(k)\|^2 \lambda^{i-1} \sum_{m=0}^{i-1} E\{[\Delta \cos \theta_m(k)]^2\} \\ &\quad + \sum_{j=0}^{i-1} \lambda^{i-j} \{E\{\hat{d}_{2,j}^2(k)\} E\{[\Delta \sin \theta_j(k)]^2\} + E\{[\Delta \hat{d}_{2,j}(k)]^2\} (1-\lambda)\} \\ &\quad + \sum_{j=0}^{i-1} E\{\hat{d}_{2,j}^2(k)\} (1-\lambda) \sum_{p=j+1}^{i-1} E\{[\Delta \cos \theta_p(k)]^2\} \lambda^{i-j-1} \\ &\quad + \frac{\lambda^i - 1}{\lambda - 1} \sigma_n^2, \end{aligned} \quad (9.63)$$

where σ_n^2 is the variance of $\eta_j^{bi}(k)$, whereas $E\{d^2(k)\}$ was approximated by $\sigma_x^2 \|\mathbf{w}_o(k)\|^2$ by neglecting the effects of the measurement noise in the desired signal. Vector $\mathbf{w}_o(k)$ represents the tap coefficients of the unknown model.

9.2.3.3 Mean squared value of $\Delta u_{i,i}(k)$

The value of $\Delta u_{i,i}(k)$ can be derived from (9.18) as follows:

$$\begin{aligned} \Delta u_{i,i}(k) = & \sqrt{\lambda u_{i,i}^2(k-1) + a_{i,i}^2(k)} \\ & - \sqrt{\lambda u_{i,i;Q}^2(k-1) + a_{i,i;Q}^2(k) - \eta_M[\lambda u_{i,i;Q}^2(k-1), a_{i,i;Q}^2(k)]} \\ & + \eta_S[\lambda u_{i,i;Q}^2(k-1) + a_{i,i}^2(k)] \end{aligned} \quad (9.64)$$

Considering that the equation above has a square-root operation, the following approximation can be used

$$\sqrt{r} - \sqrt{r - \Delta r} \approx \frac{\Delta r}{2\sqrt{r}}; \quad (9.65)$$

so that

$$\begin{aligned} E\{[\Delta u_{i,i}(k)]^2\} \approx & \lambda^2 E\{[\Delta u_{i,i}(k)]^2\} + (1 - \lambda) E\{[\Delta a_{i,i}(k)]^2\} \\ & + \frac{\sigma_n^2}{4\sigma_x^2} (1 - \lambda) \left[\frac{1 + \lambda}{2\lambda} \right]^i + \sigma_n^2. \end{aligned} \quad (9.66)$$

9.2.3.4 Mean square value of $\Delta \sin \theta_i(k)$

For a division operation, the following approximation is valid for small Δr

$$\frac{1}{r + \Delta r} \approx \frac{1}{r} \left[1 - \frac{\Delta r}{r} \right]. \quad (9.67)$$

In (9.20), by replacing $a_{i,i}(k)$ and $u_{i,i}(k)$, respectively, by $a_{i,i;Q}(k) + \Delta a_{i,i}(k)$ and $u_{i,i;Q}(k) + \Delta u_{i,i}(k)$, and using the approximation above, it is possible to show that

$$\Delta \sin \theta_i(k) = \frac{\Delta a_{i,i}(k)}{u_{i,i}(k)} + \frac{a_{i,i}(k)}{u_{i,i}^2(k)} \Delta u_{i,i}(k) + \eta_D(k), \quad (9.68)$$

where $\eta_D(k)$ represents $\eta_D[a_{i,i;Q}(k), u_{i,i;Q}(k)]$. Now, considering that the instantaneous and accumulated errors are zero mean and with relatively small cross-correlations, and using the averaging principle, it can be demonstrated that

$$\begin{aligned} E\{[\Delta \sin \theta_i(k)]^2\} \approx & \frac{E\{[\Delta a_{i,i}(k)]^2\} \{(1 - \lambda)^3 + (1 - \lambda)\}}{\sigma_x^2} \left[\frac{1 + \lambda}{2\lambda} \right]^i \\ & + \frac{E\{[\Delta u_{i,i}(k)]^2\} \lambda^2 (1 - \lambda)^2}{\sigma_x^2} \left[\frac{1 + \lambda}{2\lambda} \right]^i \\ & + \frac{(1 - \lambda)^3 \sigma_n^2}{4\sigma_x^4} \left[\frac{1 + \lambda}{2\lambda} \right]^{2i} \\ & + \frac{\sigma_n^2 (1 - \lambda)^2}{\sigma_x^2} \left[\frac{1 + \lambda}{2\lambda} \right]^i + \sigma_n^2. \end{aligned} \quad (9.69)$$

9.2.3.5 Mean squared value of $\Delta \cos \theta_i(k)$

The cosines of the Givens rotations in the infinite and finite-precision implementations of the QRD-RLS algorithm are respectively expressed by

$$\begin{aligned} \cos \theta_i(k) &= \frac{\lambda^{1/2} u_{i,i;Q}(k-1)}{u_{i,i;Q}(k)} + \frac{\lambda^{1/2} \Delta u_{i,i}(k-1)}{u_{i,i;Q}(k)} \\ &\quad - \frac{\lambda^{1/2} u_{i,i;Q}(k-1)}{u_{i,i;Q}^2(k)} \Delta u_{i,i}(k) \end{aligned} \quad (9.70)$$

and

$$\cos_Q \theta_i(k) = \frac{\lambda^{1/2} u_{i,i;Q}(k-1)}{u_{i,i;Q}(k)} - \eta_D(k), \quad (9.71)$$

where $\eta_D(k)$ represents $\eta_D[\lambda^{1/2} u_{i,i;Q}(k-1), u_{i,i;Q}(k)]$. With these equations, one can show that

$$\Delta \cos \theta_i(k) = \frac{\lambda^{1/2} \Delta u_{i,i}(k-1)}{u_{i,i}(k)} - \frac{\lambda^{1/2} u_{i,i}(k-1)}{u_{i,i}^2(k)} \Delta u_{i,i}(k) + \eta_D(k). \quad (9.72)$$

Thus, if we take the squared value of (9.72) and apply the expected value operation to the resulting equation, we obtain

$$\begin{aligned} E\{[\Delta \cos \theta_i(k)]^2\} &\approx \lambda \frac{E\{[\Delta u_{i,i}(k-1)]^2\}}{E\{u_{i,i}^2(k)\}} + \lambda \frac{E\{[\Delta u_{i,i}(k)]^2\}}{E\{u_{i,i}^2(k)\}} \\ &\quad - 2\lambda \frac{E\{\Delta u_{i,i}(k-1) \Delta u_{i,i}(k)\}}{E\{u_{i,i}^2(k)\}} + E\{\eta_D^2(k)\}. \end{aligned} \quad (9.73)$$

It should be noted that $\Delta u_{i,i}(k-1)$ and $\Delta u_{i,i}(k)$ are not uncorrelated and that the mean of their product can be calculated as

$$\begin{aligned} E\{\Delta u_{i,i}(k-1) \Delta u_{i,i}(k)\} &\approx E\left\{\lambda \frac{u_{i,i}(k-1)}{u_{i,i}(k)} [\Delta u_{i,i}(k-1)]^2\right\} \\ &\approx \lambda E\{[\Delta u_{i,i}(k-1)]^2\} \\ &= \lambda E\{[\Delta u_{i,i}(k)]^2\}. \end{aligned} \quad (9.74)$$

From (9.73), (9.74), and (9.66) we get

$$\begin{aligned}
E\{[\Delta \cos \theta_i(k)]^2\} &\approx \frac{\lambda(1-\lambda)^3 E\{[\Delta u_{i,i}(k)]^2\}}{\sigma_x^2} \left[\frac{1+\lambda}{2\lambda}\right]^i \\
&+ \frac{\lambda(1-\lambda)^2 E\{[\Delta a_{i,i}(k)]^2\}}{\sigma_x^2} \left[\frac{1+\lambda}{2\lambda}\right]^i + \sigma_n^2 \\
&+ \frac{\lambda(1-\lambda)^2 \sigma_n^2}{4\sigma_x^4} \left[\frac{1+\lambda}{2\lambda}\right]^{2i} + \frac{\lambda(1-\lambda)\sigma_n^2}{\sigma_x^2} \left[\frac{1+\lambda}{2\lambda}\right]^i. \quad (9.75)
\end{aligned}$$

9.2.3.6 Mean squared value of $\Delta u_{i,j}(k)$

For the infinite-precision implementation of the QRD-RLS algorithm, the elements of the triangularized matrix $\mathbf{U}(k)$ are calculated by

$$\begin{aligned}
u_{i,j}(k) &= \lambda^{1/2} u_{i,j}(k-1) \cos \theta_i(k) + a_{i,j}(k) \sin \theta_i(k) \quad (9.76) \\
&= [\lambda^{1/2} u_{i,j;Q}(k-1) + \lambda^{1/2} \Delta u_{i,j}(k-1)] [\cos_Q \theta_i(k) + \Delta \cos \theta_i(k)] \\
&\quad + [a_{i,j;Q}(k) + \Delta a_{i,j}(k)] [\sin_Q \theta_i(k) + \Delta \sin \theta_i(k)] \\
&= \lambda^{1/2} u_{i,j;Q}(k-1) \cos_Q \theta_i(k) + a_{i,j;Q}(k) \sin_Q \theta_i(k) \\
&\quad + \lambda^{1/2} \Delta u_{i,j}(k-1) \cos_Q \theta_i(k) \\
&\quad + \lambda^{1/2} u_{i,j;Q}(k-1) \Delta \cos \theta_i(k) \\
&\quad + a_{i,j;Q}(k) \Delta \sin \theta_i(k) + \Delta a_{i,j}(k) \sin_Q \theta_i(k). \quad (9.77)
\end{aligned}$$

In finite-precision implementation the elements of $\mathbf{U}_Q(k)$ are given by

$$\begin{aligned}
u_{i,j;Q}(k) &= \lambda^{1/2} u_{i,j;Q}(k-1) \cos_Q \theta_i(k) \\
&\quad + a_{i,j;Q}(k) \sin_Q \theta_i(k) - \eta_M(k), \quad (9.78)
\end{aligned}$$

where $\eta_M(k)$ represents $\eta_M[(\lambda^{1/2} u_{i,j;Q}(k-1), \cos_Q \theta_i(k)); (a_{i,j;Q}(k), \sin_Q \theta_i(k))]$. Subtracting (9.77) from (9.78), and replacing the quantities in finite precision by their infinite precision counterpart, we obtain

$$\begin{aligned}
\Delta u_{i,j}(k) &= \lambda^{1/2} \Delta u_{i,j}(k-1) \cos \theta_i(k) + \lambda^{1/2} u_{i,j}(k-1) \Delta \cos \theta_i(k) \\
&\quad + a_{i,j}(k) \Delta \sin \theta_i(k) + \Delta a_{i,j}(k) \sin \theta_i(k) + \eta_M(k). \quad (9.79)
\end{aligned}$$

Assuming that $\eta_M(k)$ as well as the accumulated errors are zero mean with relatively small cross-correlations, then

$$\begin{aligned}
E\{[\Delta u_{i,j}(k)]^2\} &\approx \lambda E\{[\Delta u_{i,j}(k-1)]^2\} E\{\cos^2 \theta_i(k)\} \\
&\quad + \lambda E\{u_{i,j}^2(k-1)\} E\{[\Delta \cos \theta_i(k)]^2\} \\
&\quad + E\{a_{i,j}^2(k)\} E\{[\Delta \sin \theta_i(k)]^2\} \\
&\quad + E\{[\Delta a_{i,j}(k)]^2\} E\{\sin^2 \theta_i(k)\} + E\{\eta_M^2(k)\}. \quad (9.80)
\end{aligned}$$

Using (9.22) and (9.21), in the steady-state we get

$$\begin{aligned}
 E\{[\Delta u_{i,j}(k)]^2\} &\approx \frac{\lambda E\{u_{i,j}^2(k-1)\}E\{[\Delta \cos \theta_i(k)]^2\}}{1-\lambda^2} \\
 &+ \frac{E\{a_{i,j}^2(k)\}E\{[\Delta \sin \theta_i(k)]^2\}}{1-\lambda^2} \\
 &+ \frac{E\{[\Delta a_{i,j}(k)]^2\}}{1+\lambda} + \frac{E\{\eta_M^2(k)\}}{1-\lambda^2}. \tag{9.81}
 \end{aligned}$$

The equation above can be simplified into two different ways. For $i \neq j$, we can apply (9.23) and (9.27) resulting in

$$\begin{aligned}
 E\{[\Delta u_{i,j}(k)]^2\} &\approx \frac{\lambda \sigma_x^2 E\{[\Delta \cos \theta_i(k)]^2\}}{(1-\lambda)(1-\lambda^2)} \left[\frac{2\lambda}{1+\lambda} \right]^i \\
 &+ \frac{\sigma_x^2 E\{[\Delta \sin \theta_i(k)]^2\}}{1-\lambda^2} \left[\frac{2\lambda}{1+\lambda} \right]^i \\
 &+ \frac{E\{[\Delta a_{i,j}(k)]^2\}}{1+\lambda} + \frac{\sigma_n^2}{1-\lambda^2}, \tag{9.82}
 \end{aligned}$$

where σ_n^2 here is the variance of $\eta_M(k)$. For $i = j$, we have to substitute (9.69), (9.75), (9.23), and (9.24) in (9.81) in order to derive, after some manipulation

$$\begin{aligned}
 E\{[\Delta u_{i,i}(k)]^2\} &\approx \frac{2\lambda^2 - 2\lambda + 3}{2\lambda^2 - \lambda + 1} E\{[\Delta a_{i,i}(k)]^2\} \\
 &+ \frac{3\lambda^2 - 4\lambda + 2}{2\lambda^2 - \lambda + 1} \frac{\sigma_n^2}{4\sigma_x^2} \left[\frac{2\lambda}{1+\lambda} \right]^i \\
 &+ \frac{(2\lambda^2 - 2\lambda + 2)\sigma_n^2}{(2\lambda^2 - \lambda + 1)(1-\lambda)} \\
 &+ \frac{\sigma_n^2 \sigma_x^2}{(1-\lambda)^2(2\lambda^2 - \lambda + 1)} \left[\frac{1+\lambda}{2\lambda} \right]^i. \tag{9.83}
 \end{aligned}$$

9.2.3.7 Mean squared value of $\Delta \hat{d}_{2,i}(k)$

The elements of vector $\hat{\mathbf{d}}_2(k)$ are resultant of the application of $N+1$ Givens rotations to $\lambda^{1/2} \mathbf{d}_2(k-1)$, that is

$$\hat{d}_{2,i}(k) = \lambda^{1/2} \hat{d}_{2,i}(k-1) \cos \theta_i(k) + b_i(k) \sin \theta_i(k). \tag{9.84}$$

This equation is similar to (9.76); as a consequence, by following the same steps to derive (9.79), we can show that

$$\begin{aligned}
 E\{[\Delta \hat{d}_{2,i}(k)]^2\} &\approx \frac{\lambda E\{d_{2,i}^2(k)\}E\{[\Delta \cos \theta_i(k)]^2\}}{1 - \lambda^2} \\
 &+ \frac{E\{b_i^2(k)\}E\{[\Delta \sin \theta_i(k)]^2\}}{1 - \lambda^2} \\
 &+ \frac{E\{[\Delta b_i(k)]^2\}}{1 + \lambda} + \frac{\sigma_n^2}{1 - \lambda^2}.
 \end{aligned} \tag{9.85}$$

9.2.3.8 Mean squared value of $\Delta e(k)$

The error signal in the infinite- and finite-precision implementations are given by

$$e(k) = e_q(k) \cos \theta_N(k) \cdots \cos \theta_0(k) \tag{9.86}$$

and

$$e_Q(k) = Q[e_{q;Q}(k)Q[\cos_Q \theta_0(k) \cdots Q[\cos_Q \theta_N(k) \cos_Q \theta_{N-1}(k)] \cdots]], \tag{9.87}$$

respectively.

From (9.47), the *a posteriori* error signal $e(k)$ can be expressed as

$$\begin{aligned}
 e(k) &= [e_{q;Q}(k) + \Delta e_q(k)][\cos \theta_N(k) + \Delta \cos \theta_N(k)] \cdots \\
 &[\cos_Q \theta_1(k) + \Delta \cos \theta_1(k)][\cos_Q \theta_0(k) + \Delta \cos \theta_0(k)] \\
 &= e_{q;Q}(k) \cos_Q \theta_N(k) \cdots \cos_Q \theta_0(k) + \Delta e_q(k) \cos \theta_N(k) \cdots \cos \theta_0(k) \\
 &+ e_{q;Q}(k) \left[\sum_{i=0}^N \Delta \cos_Q \theta_i(k) \prod_{\substack{j=0 \\ i \neq j}}^N \cos \theta_j(k) \right] \\
 &+ \Delta e_{q;Q}(k) \cos_Q \theta_N(k) \cdots \cos_Q \theta_0(k),
 \end{aligned} \tag{9.88}$$

where, in the last expression, the error terms of the second and higher order were ignored.

The application of (9.41) to the multiplication operations of (9.16) yields

$$\begin{aligned}
 e_Q(k) &\approx e_{q;Q}(k) \cos_Q \theta_N(k) \cos_Q \theta_{N-1}(k) \cdots \cos_Q \theta_1(k) \cos_Q \theta_0(k) \\
 &- e_{q;Q}(k) \left[\sum_{i=0}^N \prod_{j=i+1}^N \cos_Q \theta_j(k) \eta_i^e(k) \right] - \eta_{N+1}^e(k).
 \end{aligned} \tag{9.89}$$

By replacing (9.88) and (9.89) in the definition (9.47), $\Delta e(k)$ results in

$$\begin{aligned} \Delta e(k) \approx & e_{q;Q}(k) \left[\sum_{i=0}^N \Delta \cos \theta_i(k) \prod_{\substack{j=0 \\ i \neq j}}^N \cos \theta_j(k) \right] \\ & + \Delta e_{q;Q}(k) \cos_Q \theta_0(k) \cdots \cos_Q \theta_N(k) \\ & + e_{q;Q}(k) \left[\sum_{i=0}^N \prod_{j=i+1}^N \cos_Q \theta_j(k) \eta_i^e(k) \right] - \eta_{N+1}^e(k). \end{aligned} \quad (9.90)$$

We assume that $\Delta e_{q;Q}(k)$, $e_q(k)$, $\Delta \cos \theta_i(k)$, and $\eta_i^e(k)$, for $i = 0, \dots, N+1$, are all zero mean with relatively small cross-correlation between each other. Also, the variance $\eta_i^e(k)$ is considered to be σ_n^2 (that is the variance of the quantization noise), and $E\{\cos^2 \theta_i(k)\} \approx \lambda$.

With the above assumptions, one can show that the expected value of the accumulated quantization error in the *a posteriori* error signal is given by

$$\begin{aligned} E\{[\Delta e(k)]^2\} \approx & E\{e_{q;Q}^2(k)\} \left[\sum_{i=0}^N E\{[\Delta \cos \theta_i(k)]^2\} \lambda^N \right] \\ & + E\{[\Delta e_q(k)]^2\} \lambda^{N+1} + E\{e_{q;Q}^2(k)\} \sum_{i=0}^N \lambda^{N-i} \sigma_n^2 + \sigma_n^2. \end{aligned} \quad (9.91)$$

In the first term of the right-hand-side of the equation above, we can substitute $E\{e_q^2(k)\}$ as suggested in (9.35). In the third term, (9.35) should also be applied. In the second term, if it is noted that $e_q(k)$ is the first element of $\mathbf{d}_2(k)$, from (9.63), we can determine $E\{[\Delta e_q(k)]^2\}$ by setting $i = N+1$, i.e.,

$$\begin{aligned} E\{[\Delta e_q(k)]^2\} \approx & \sigma_x^2 \|\mathbf{w}_o(k)\|^2 \lambda^N \sum_{m=0}^N E\{[\Delta \cos \theta_m(k)]^2\} \\ & + \sum_{j=0}^N \lambda^{N+1-j} [E\{\hat{d}_{2,j}^2(k)\} E\{[\Delta \sin \theta_j(k)]^2\} + E\{[\Delta \hat{d}_{2,j}(k)]^2\} (1-\lambda)] \\ & + \sum_{j=0}^N E\{\hat{d}_{2,j}^2(k)\} (1-\lambda) \sum_{p=j+1}^N E\{[\Delta \cos \theta_p(k)]^2\} \lambda^{N-j} \\ & + \frac{\lambda^{N+1} - 1}{\lambda - 1} \sigma_n^2. \end{aligned} \quad (9.92)$$

9.2.3.9 Mean squared value of $\Delta w_i(k)$

The tap coefficients of the adaptive filter in the QRD-RLS algorithm are calculated through the back-substitution algorithm, as illustrated in (9.14) and (9.15). After some manipulations, it can be shown that

$$\Delta w_i(k) = \frac{\hat{d}_{2,i}(k) - \sum_{j=i+1}^N w_i(k) u_{i,j}(k)}{u_{i,i}(k)} - \frac{\hat{d}_{2,i;Q}(k) - \sum_{j=i+1}^N w_{i;Q}(k) u_{i,j;Q}(k) + \eta_M(k)}{u_{i,i;Q}(k)} + \eta_D(k), \quad (9.93)$$

where in the above equation we have

$$\eta_M(k) \triangleq \eta_M \left[\sum_{j=i+1}^N w_{i;Q}(k) u_{i,j;Q}(k) \right] \quad (9.94)$$

and

$$\eta_D(k) \triangleq \eta_D \left[\left(\hat{d}_{2,i;Q}(k) - \sum_{j=i+1}^N w_{i;Q}(k) u_{i,j;Q}(k) + \eta_8(k) \right), u_{i,i;Q}(k) \right]. \quad (9.95)$$

From the expression above and using the approximation in (9.67), we obtain

$$\Delta w_i(k) \approx \frac{\Delta \hat{d}_{2,i}(k) - \sum_{j=i+1}^N [w_{j;Q}(k) \Delta u_{i,j}(k) + \Delta w_j(k) u_{i,j;Q}(k)]}{u_{i,i;Q}(k)} - \frac{w_{i;Q}(k) \Delta u_{i,i}(k)}{u_{i,i;Q}(k)} + \frac{\eta_M(k)}{u_{i,i;Q}(k)} + \eta_D(k), \quad (9.96)$$

where, in the last expression, we replaced the finite-precision quantities by their infinite-precision counterparts. The introduced errors are of second order, and can therefore be neglected. Assuming that $\eta_M(k)$ and $\eta_D(k)$ are uncorrelated and zero mean; employing the averaging principle [9], it can be shown that

$$\begin{aligned} E\{[\Delta w_i(k)]^2\} &\approx \frac{E\{[\Delta \hat{d}_{2,i}(k)]^2\}}{E\{u_{i,i}^2(k)\}} + \frac{\sum_{j=i}^N E\{w_j^2(k)\} E\{[\Delta u_{i,j}(k)]^2\}}{E\{u_{i,i}^2(k)\}} \\ &\quad + \frac{\sum_{j=i+1}^N E\{[\Delta w_j(k)]^2\} E\{u_{i,j}^2(k)\}}{E\{u_{i,i}^2(k)\}} \\ &\quad + \frac{\sigma_n^2}{E\{u_{i,i}^2(k)\}} + \sigma_n^2. \end{aligned} \quad (9.97)$$

In order to calculate $E\{[\Delta w_i(k)]^2\}$, it is necessary to have $E\{[\Delta u_{i,j}(k)]^2\}$ and $E\{[\Delta d_{2,i}(k)]^2\}$, that in turn require the values of $E\{[\Delta a_{i,i}(k)]^2\}$, $E\{[\Delta b_i(k)]^2\}$, $E\{[\Delta u_{i,i}(k)]^2\}$, $E\{[\Delta \sin \theta_i(k)]^2\}$, and $E\{[\Delta \cos \theta_i(k)]^2\}$.

From (9.97), we can determine the mean of the squared norm of the deviation in the tap coefficients as follows:

$$E\{\|\Delta\mathbf{w}(k)\|^2\} = \sum_{i=0}^N E\{[\Delta w_i(k)]^2\} \tag{9.98}$$

9.2.4 Simulation results

The derived equations were verified through simulations using a system identification application where both input signal and measurement noise were pseudo-random sequences with normal distribution and zero-mean. Four different moving-averaging processes were utilized to emulate unknown systems with orders equal to 4, 6, 8, and 10, respectively. In all simulations, the QRD-RLS algorithm ran for 1500 iterations and the simulation results were obtained by averaging the results of 100 independent runs. Infinite-precision simulations were executed with 64 bits floating-point arithmetic. In the fixed-point implementation, the quantities were represented by numbers with magnitude less than unity. Frequent overflow was avoided by choosing the input signal variance appropriately.

The first experiment was aimed to verify the results for different moving average processes. The input signal variance was fixed at -30 dB, while the additional noise variance was -70 dB. The forgetting factor was $\lambda = 0.95$ and the wordlength was 15 bits. The measured and calculated results for $E\{\|\mathbf{w}(k)\|_2^2\}$ and $E\{[\Delta e(k)]^2\}$ are presented in Table 9.2, and it can be seen that simulated and calculated values are in close agreement.

Table 9.2 Fixed-point environment: simulations for distinct MA processes with 15 bits and forgetting factor $\lambda = 0.95$.

MA process	$E\{\ \Delta\mathbf{w}(k)\ _2^2\}$ (dB)		$E\{[\Delta e(k)]^2\}$ (dB)	
	Simulated	Calculated	Simulated	Calculated
MA1	-64.7	-64.3	-92.6	-92.2
MA2	-62.7	-62.2	-91.7	-91.3
MA3	-61.2	-60.7	-91.2	-90.8
MA4	-59.9	-59.2	-90.9	-90.5

The formulas (9.91) and (9.98) were tested for different values of λ , $\sigma_x^2 = -25$ dB and $\sigma_r^2 = -70$ dB. The wordlength again was 15 bits. The results are presented in Table 9.3. Again, we observe close agreement between the calculated and simulated values.

Table 9.3 Simulations for distinct λ .

Forgetting factor (λ)	$E\{\ \Delta\mathbf{w}(k)\ _2^2\}$ (dB)		$E\{[\Delta e(k)]^2\}$ (dB)	
	Simulated	Calculated	Simulated	Calculated
0.90	-68.2	-67.7	-93.7	-93.2
0.93	-69.0	-68.7	-93.0	-92.6
0.95	-69.7	-69.3	-92.5	-92.2
0.97	-70.3	-70.1	-92.1	-91.8
0.99	-70.9	-70.7	-91.6	-91.3

The theoretical results were also verified for different wordlengths with $\sigma_x^2 = -30$ dB, $\lambda = 0.95$ and $\sigma_r^2 = -70$ dB. Table 9.4 illustrates the results. As can be noted in the current and in all previous experiments, the obtained formulas are shown to model accurately the finite wordlength effects in the main quantities of the QRD-RLS algorithm.

Table 9.4 Simulations for distinct precisions.

Number of bits	$E\{\ \Delta\mathbf{w}(k)\ _2^2\}$ (dB)		$E\{[\Delta e(k)]^2\}$ (dB)	
	Simulated	Calculated	Simulated	Calculated
12	-46.5	-46.3	-74.1	-74.1
15	-68.2	-64.3	-91.7	-92.2
20	-94.8	-94.4	-122.3	-122.3
25	-124.9	-124.6	-152.8	-152.4
30	-154.0	-154.7	-182.8	-182.5

9.3 Precision Analysis of the Fast QRD-Lattice Algorithm

This section discusses the finite-precision analysis for the FQRD-lattice algorithm proposed by McWhirter [10]. The notation of this reference was followed. The C Language pseudo-code for the FQRD-lattice algorithm is shown in Table 9.5, which details all algorithmic steps labeled from step (S.1) through (S.18). It can be seen that this algorithm takes advantage of two operations named *rotor* and *cisor* for performing all internal computations.

Exploring the fact that only two basic operations are performed by this algorithm, a very regular structure can be derived as shown in Figure 9.1. This figure uses squares to represent *rotor* cells (that perform rotations) and circles to represent *cisor* cells (that perform cosine/sine calculations). The small cells in the last stage represent multipliers.

Table 9.5 C Language pseudo-code for the FQRD-lattice algorithm.

FQRD-Lattice RLS [10]

```

void rotor (double  $x_{in}$ , double  $y_{in}$ , double  $x_{out}$ , double  $y_{out}$ , double  $c_{in}$ , double  $s_{in}$ )
{
     $x_{out} = Q[\lambda^{1/2}x_{in}c_{in} + y_{in}s_{in}];$  (S.1)
     $y_{out} = Q[-\lambda^{1/2}x_{in}s_{in} + y_{in}c_{in}];$  (S.2)
}

void cisor (double  $x_{in}$ , double  $y_{in}$ , double  $x_{out}$ , double  $b_{in}$ , double  $b_{out}$ , double  $c_{out}$ ,
double  $s_{out}$ )
{
    double aux;

     $x_{out} = Q[\sqrt{Q[\lambda x_{in}^2 + y_{in}^2]}];$  (S.3)
     $c_{out} = Q[\lambda^{1/2}x_{in}/x_{out}];$  (S.4)
     $s_{out} = Q[y_{in}/x_{out}];$  (S.5)
     $b_{out} = Q[b_{in}c_{out}];$  (S.6)
}

void FqrdLattice (double  $x(k)$ , double  $d(k)$ , double  $e(k)$ )
{
    int i;
    double aux;

     $e_0^f(k) = e_0^b(k) = x(k);$  (S.7)
     $e_0(k) = d(k);$  (S.8)
     $\alpha_0(k) = 1.0;$  (S.9)
    for (i=1; i  $\leq$  N+1; i++)
    {
        cisor ( $\alpha_{i-1}^b(k-1)$ ,  $e_{i-1}^b(k)$ ,  $\alpha_{i-1}^f(k)$ ,  $\alpha_{i-1}(k)$ ,  $\alpha_i(k)$ ,  $c_i^f(k)$ ,  $s_i^f(k)$ ); (S.10)
        rotor ( $\beta_{i-1}^f(k-1)$ ,  $e_{i-1}^f(k)$ ,  $\beta_{i-1}^b(k)$ ,  $e_i^f(k)$ ,  $c_i^f(k-1)$ ,  $s_i^f(k-1)$ ); (S.11)
        rotor ( $\beta_{i-1}(k-1)$ ,  $e_{i-1}(k)$ ,  $\beta_{i-1}(k)$ ,  $e_i(k)$ ,  $c_i^f(k)$ ,  $s_i^f(k)$ ); (S.12)
         $\varepsilon_i^f(k) = Q[\alpha_i(k-1)e_i^f(k)];$  (S.13)
         $\varepsilon_i(k) = Q[\alpha_i(k)e_i(k)];$  (S.14)
        cisor ( $\alpha_{i-1}^f(k-1)$ ,  $e_{i-1}^f(k)$ ,  $\alpha_{i-1}^b(k)$ ,  $aux$ ,  $aux$ ,  $c_i^b(k)$ ,  $s_i^b(k)$ ); (S.15)
        rotor ( $\beta_{i-1}^b(k-2)$ ,  $e_{i-1}^b(k)$ ,  $\beta_{i-1}^f(k-1)$ ,  $e_i^b(k)$ ,  $c_i^b(k)$ ,  $s_i^b(k)$ ); (S.16)
         $\varepsilon_i^b(k) = Q[\alpha_i(k)e_i^b(k)];$  (S.17)
    }
     $e(k) = Q[\alpha_{N+1}(k)e_{N+1}(k)];$  (S.18)
}

```

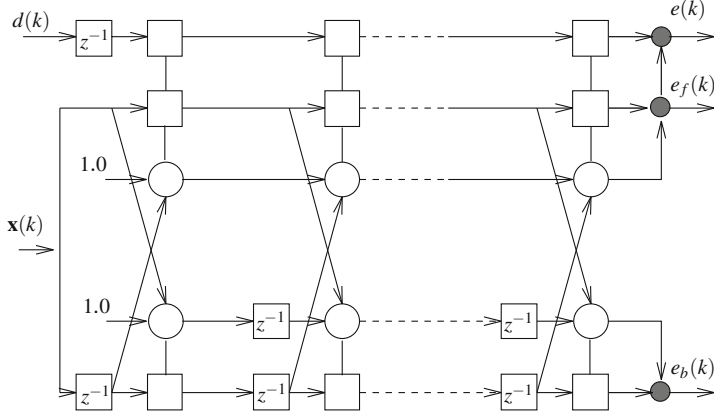


Fig. 9.1 Structure representing the FQRD-lattice algorithm.

9.3.1 Infinite-precision analysis

This section derives mean squared values of the internal variables in the FQRD-lattice algorithm. They are of key importance for the finite-precision analysis that will be performed in the next subsection.

9.3.1.1 Mean squared values of $c_i^f(k)$ and $s_i^f(k)$

Previous studies [11] have shown that the mean squared values of the forward recursion cosines and sines are

$$E\{[c_i^f(k)]^2\} = \lambda, \text{ and} \tag{9.99}$$

$$E\{[s_i^f(k)]^2\} = 1 - \lambda. \tag{9.100}$$

Simulations for these variables in the QRD-RLS and for the FQRD-lattice algorithms indicate that these approximations are reasonable.

9.3.1.2 Mean squared values of $\beta_i^f(k)$, $e_i^f(k)$, and $\alpha_i^f(k)$

Step (S.11) of the FQRD-lattice algorithm implies that

$$\beta_i^f(k) = \lambda^{1/2} c_i^f(k-1) \beta_{i-1}^f(k-1) + s_i^f(k-1) e_{i-1}^f(k), \text{ and} \tag{9.101}$$

$$e_i^f(k) = -\lambda^{1/2} s_i^f(k-1) \beta_{i-1}^f(k-1) + c_i^f(k-1) e_{i-1}^f(k). \tag{9.102}$$

If it is supposed that the sines and cosines of the previous equations are uncorrelated with each other, and that the values of the sines are zero-mean, then it is possible to obtain the following relations:

$$E\{[\beta_i^f(k)]^2\} = \lambda E\{[c_i^f(k-1)]^2\} E\{[\beta_{i-1}^f(k-1)]^2\} + E\{[s_i^f(k-1)]^2\} E\{[e_{i-1}^f(k)]^2\}, \quad (9.103)$$

$$E\{[e_i^f(k)]^2\} = \lambda E\{[s_i^f(k)]^2\} E\{[\beta_{i-1}^f(k)]^2\} + E\{[c_i^f(k)]^2\} E\{[e_{i-1}^f(k)]^2\}. \quad (9.104)$$

Substituting relations (9.99) and (9.100) in (9.103), it is possible to show that

$$E\{[\beta_{i-1}^f(k)]^2\} = \frac{E\{[e_{i-1}^f(k)]^2\}}{1 + \lambda}. \quad (9.105)$$

Substituting relations (9.99), (9.100), and (9.105) on (9.104), we obtain

$$E\{[e_i^f(k)]^2\} = \frac{2\lambda}{1 + \lambda} E\{[e_{i-1}^f(k)]^2\}. \quad (9.106)$$

Since $e_0^f(k) = x(k)$, according to step (S.10), it follows that

$$E\{[e_i^f(k)]^2\} = \sigma_x^2 \left[\frac{2\lambda}{1 + \lambda} \right]^i. \quad (9.107)$$

Consequently, according to (9.105),

$$E\{[\beta_i^f(k)]^2\} = \frac{\sigma_x^2}{1 + \lambda} \left[\frac{2\lambda}{1 + \lambda} \right]^i. \quad (9.108)$$

The recursion formula for $\alpha_{i-1}^f(k)$ is given by

$$\alpha_{i-1}^f(k) = \sqrt{\lambda [\alpha_{i-1}^b(k-1)]^2 + [e_{i-1}^f(k)]^2}, \quad (9.109)$$

according to step (S.15). Supposing that $\alpha_{i-1}^f(k)$ and $e_{i-1}^f(k)$ are stationary for $k \rightarrow \infty$, it follows that

$$E\{[\alpha_i^f(k)]^2\} = \frac{E\{[e_i^f(k)]^2\}}{1 - \lambda}. \quad (9.110)$$

Using (9.107), the following expression results:

$$E\{[\alpha_i^f(k)]^2\} = \frac{\sigma_x^2}{1-\lambda} \left[\frac{2\lambda}{1+\lambda} \right]^i. \quad (9.111)$$

9.3.1.3 Mean squared values of $c_i^b(k)$ and $s_i^b(k)$

According to the algorithm step (S.15), it follows that sines and cosines are calculated by

$$c_i^b(k) = \frac{\lambda^{1/2} \alpha_{i-1}^f(k-1)}{\alpha_{i-1}^f(k)}, \text{ and} \quad (9.112)$$

$$s_i^b(k) = \frac{e_{i-1}^f(k)}{\alpha_{i-1}^f(k)}. \quad (9.113)$$

Thus, the mean squared values of the backward recursion sines and cosines are

$$E\{[c_i^b(k)]^2\} = \frac{\lambda E\{[\alpha_{i-1}^f(k-1)]^2\}}{E\{[\alpha_{i-1}^f(k)]^2\}}, \text{ and} \quad (9.114)$$

$$E\{[s_i^b(k)]^2\} = \frac{E\{[e_{i-1}^f(k)]^2\}}{E\{[\alpha_{i-1}^f(k)]^2\}}. \quad (9.115)$$

In the above equations, the averaging principle [9] was used. Considering that $\alpha_{i-1}^f(k)$ is statistically stationary as $k \rightarrow \infty$ and using the fundamental trigonometric relation, it follows

$$E\{[c_i^b(k)]^2\} = \lambda, \quad (9.116)$$

$$E\{[s_i^b(k)]^2\} = 1 - \lambda. \quad (9.117)$$

Surprisingly, these mean square values are the same as the ones for the forward recursion sines and cosines, and different from those in the fast QRD-RLS proposed by Bellanger [10, 12].

9.3.1.4 Mean squared values of $\beta_i^b(k)$, $e_i^b(k)$, and $\alpha_i^b(k)$

The relations for $\beta_i^b(k)$ and $e_i^b(k)$ derived from step (S.16) are totally analogous to the ones for $\beta_i^f(k)$ and $e_i^f(k)$ shown in (9.101) and (9.102). Considering that the

mean squared values for cosines and sines are the same in the backward and forward rotations and using the same statistical independence assumptions, it is possible to obtain the following expressions:

$$E\{[e_i^b(k)]^2\} = \sigma_x^2 \left[\frac{2\lambda}{1+\lambda} \right]^i \quad (9.118)$$

$$E\{[\beta_i^b(k)]^2\} = \frac{\sigma_x^2}{1+\lambda} \left[\frac{2\lambda}{1+\lambda} \right]^i \quad (9.119)$$

$$E\{[\alpha_i^b(k)]^2\} = \frac{\sigma_x^2}{1-\lambda} \left[\frac{2\lambda}{1+\lambda} \right]^i. \quad (9.120)$$

9.3.1.5 Mean squared values of $\beta_i(k)$ and $e_i(k)$

Using properties of the triangularized input signal matrix [11], a very simple relationship for the mean square value of $\beta_i(k)$ can be derived. It is supposed that the reference input $d(k)$ is an MA process added with white Gaussian measurement noise $r(k)$ so that $d(k) = w^o(k) * x(k) + r(k)$. In this case, $w^o(k)$ is a sequence with the coefficients of the MA process with non-zero values for $k = 0, \dots, N$.

$$E\{\beta_i^2(k)\} = \left[\frac{2\lambda}{1+\lambda} \right]^i \left[\frac{\sigma_x^2}{1-\lambda} [w_i^o]^2 + \frac{\sigma_x^2}{1+\lambda} \sum_{j=i+1}^N [w_j^o]^2 \right] \quad (9.121)$$

Using the norm conservation property of Givens rotations, a relation between $E\{e_i^2(k)\}$ and $E\{\beta_i^2(k)\}$ can be derived as follows:

$$E\{e_i^2(k)\} = \sigma_x^2 \|\mathbf{w}^o\|^2 + (\lambda - 1) \sum_{j=0}^{i-1} E\{\beta_j^2(k)\}, \quad (9.122)$$

where \mathbf{w}^o is a vector with $N + 1$ entries with the sequence $w^o(k)$, $k = 0, \dots, N$.

9.3.2 Finite-precision analysis

9.3.2.1 Mean squared value of $\Delta\alpha_i^b(k)$

According to step (S.10), the finite-precision version of $\alpha_i^b(k)$, denoted by $\alpha_{i;Q}^b(k)$, can be modeled as

$$\alpha_{i-1;Q}^b(k) = \sqrt{\lambda [\alpha_{i-1;Q}^b(k-1)]^2 + [e_{i-1;Q}^f(k)]^2 + \eta_M(k)} + \eta_S(k), \quad (9.123)$$

where $\eta_M(k)$ and $\eta_S(k)$ are instantaneous quantization errors due to multiplication and square-root operations. Considering only first order terms, it is possible to obtain

$$\begin{aligned} \Delta \alpha_{i-1}^b(k) &= \frac{\lambda \alpha_{i-1}^b(k-1) \Delta \alpha_{i-1}^b(k-1) + e_{i-1}^b(k) \Delta e_{i-1}^b(k)}{\alpha_{i-1}^b(k)} \\ &\quad - \frac{\eta_M(k)}{\alpha_{i-1}^b(k)} + \eta_S(k). \end{aligned} \quad (9.124)$$

Squaring the above equation, supposing that the deviations and instantaneous quantization noises are all zero mean and uncorrelated with each other, and substituting Equations (9.118) and (9.120) it follows that

$$\begin{aligned} E\{[\Delta \alpha_{i-1}^b(k)]^2\} &= \frac{E[\Delta e_{i-1}^b(k)]^2}{1+\lambda} + \frac{\sigma_n^2}{4\sigma_x^2} \frac{1}{1+\lambda} \left[\frac{1+\lambda}{2\lambda} \right]^{i-1} \\ &\quad + \frac{\sigma_n^2}{1-\lambda^2}. \end{aligned} \quad (9.125)$$

The averaging principle [9] was used on the derivation.

9.3.2.2 Mean squared values of $\Delta s_i^f(k)$ and $\Delta c_i^f(k)$

Using relations derived from step (S.15) and first-order approximations it is possible to write

$$E\{[\Delta s_i^f(k)]^2\} = E \left[\frac{\Delta e_{i-1}^b(k)}{\alpha_{i-1}^b(k)} - \frac{e_{i-1}^b(k) \Delta \alpha_{i-1}^b(k)}{[\alpha_{i-1}^b(k)]^2} + \eta_D(k) \right]^2. \quad (9.126)$$

Using only first-order terms, supposing that the deviations and quantization noise are all zero mean and uncorrelated with each other, and using the averaging principle [9], it is possible to derive

$$\begin{aligned} E\{[\Delta s_i^f(k)]^2\} &= \frac{E[\Delta e_{i-1}^b(k)]^2}{\sigma_x^2} (1-\lambda) \left[\frac{1+\lambda}{2\lambda} \right]^{i-1} + \sigma_n^2 \\ &\quad + E\{[\Delta \alpha_{i-1}^b(k)]^2\} \sigma_x^2 (1-\lambda)^2 \left[\frac{1+\lambda}{2\lambda} \right]^{i-1}. \end{aligned} \quad (9.127)$$

The same methodology can be used to obtain the mean squared value of $\Delta c_i^f(k)$. The result is

$$E\{[\Delta c_i^f(k)]^2\} = \frac{2\lambda(1-\lambda^2)}{\sigma_x^2} \left[\frac{1+\lambda}{2\lambda} \right]^{i-1} E\{[\Delta \alpha_{i-1}^b(k)]^2\} + \sigma_n^2. \quad (9.128)$$

9.3.2.3 Mean squared values of $\Delta\beta_i^f(k)$ and $\Delta e_i^f(k)$

The evolution of $\beta_i^f(k)$ is described by (9.103). If second-order errors are neglected, it is possible to write

$$\begin{aligned}\Delta\beta_{i-1}^f(k) &= \lambda^{1/2}c_i^f(k-1)\Delta\beta_{i-1}^f(k-1) \\ &\quad + \lambda^{1/2}\Delta c_i^f(k-1)\beta_{i-1}^f(k-1) + \Delta s_i^f(k-1)e_{i-1}^f(k) \\ &\quad + s_i^f(k-1)\Delta e_{i-1}^f(k) + \eta_M(k).\end{aligned}\quad (9.129)$$

Supposing that all the deviations and the instantaneous quantization noise are zero mean and uncorrelated with each other, it is possible to get

$$\begin{aligned}E\{[\Delta\beta_{i-1}^f(k)]^2\} &= \frac{\lambda\sigma_x^2}{(1+\lambda)(1-\lambda^2)}\left[\frac{2\lambda}{1+\lambda}\right]^{i-1}E\{[\Delta c_i^f(k)]^2\} \\ &\quad + \frac{\sigma_n^2}{1-\lambda^2} + \frac{\sigma_x^2}{1-\lambda^2}\left[\frac{2\lambda}{1+\lambda}\right]^{i-1}E\{[\Delta s_i^f(k)]^2\} \\ &\quad + E\{[\Delta s_i^f(k)]^2\} + \frac{E\{[\Delta e_{i-1}^f(k)]^2\}}{1+\lambda}.\end{aligned}\quad (9.130)$$

Using Equation (9.104) and following the same steps, it can be shown that

$$\begin{aligned}E\{[\Delta e_i^f(k)]^2\} &= \sigma_x^2\left[\frac{2\lambda}{1+\lambda}\right]^{i-1}E\{[\Delta c_i^f(k)]^2\} + \lambda E\{[\Delta e_{i-1}^f(k)]^2\} \\ &\quad + E\{[\Delta s_i^f(k)]^2\}\sigma_x^2\frac{\lambda}{1+\lambda}\left[\frac{2\lambda}{1+\lambda}\right]^{i-1} \\ &\quad + \lambda(1-\lambda)E\{[\Delta s_i^f(k)]^2\} + \sigma_n^2.\end{aligned}\quad (9.131)$$

9.3.2.4 Mean squared values of $\Delta\varepsilon_i^f(k)$, $\Delta\alpha_i(k)$, and $\Delta\varepsilon_i(k)$

According to step (S.13), it is possible to write

$$\varepsilon_i^f(k) = \alpha_i(k-1)e_i^f(k).\quad (9.132)$$

Using the same methodology of previous derivations, it is possible to obtain

$$E\{[\Delta\varepsilon_i^f(k)]^2\} = \sigma_x^2\left[\frac{2\lambda}{1+\lambda}\right]^i E\{[\Delta\alpha_i(k)]^2\} + \lambda^i E\{[\Delta e_i^f(k)]^2\} + \sigma_n^2.\quad (9.133)$$

Step (S.10) implies that

$$\alpha_i(k) = c_i^f(k-1)\alpha_{i-1}(k).\quad (9.134)$$

The mean squared value for $\Delta\alpha_i(k)$ can be shown to be

$$E\{[\Delta\alpha_i(k)]^2\} = E\{[\Delta c_i^f(k)]^2\}\lambda^{i-1} + \lambda E\{[\Delta\alpha_{i-1}(k)]^2\} + \sigma_n^2. \quad (9.135)$$

It can be seen that $\varepsilon_i(k)$ is described by step (S.14). The mean squared value for $\Delta\varepsilon_i(k)$ can be calculated as

$$\begin{aligned} E\{[\Delta\varepsilon_i(k)]^2\} &= E\{[\Delta\alpha_i(k)]^2\}E\{e_i^2(k)\} + \sigma_n^2 \\ &\quad + \frac{\sigma_x^2}{1-\lambda} \left[\frac{2\lambda}{1+\lambda} \right]^{i-1} E\{[\Delta e_i(k)]^2\}. \end{aligned} \quad (9.136)$$

9.3.2.5 Mean squared values of $\Delta\alpha_i^f(k)$, $\Delta s_i^b(k)$, $\Delta c_i^f(k)$, $\Delta\beta_i(k)$, and $\Delta e_i(k)$

According to Table 9.5, these quantities have dynamic relations that are very similar to their “dual” (forward or backward) counterparts. Using the same methodology described in the previous sections, the following relations are derived:

$$\begin{aligned} E\{[\Delta\alpha_{i-1}^f(k)]^2\} &= \frac{E[\Delta e_{i-1}^f(k)]^2}{1+\lambda} + \frac{\sigma_n^2}{4\sigma_x^2} \frac{1}{1+\lambda} \left[\frac{1+\lambda}{2\lambda} \right]^{i-1} \\ &\quad + \frac{\sigma_n^2}{1-\lambda^2} \end{aligned} \quad (9.137)$$

$$\begin{aligned} E\{[\Delta s_i^b(k)]^2\} &= \frac{E[\Delta e_{i-1}^f(k)]^2}{\sigma_x^2} (1-\lambda) \left[\frac{1+\lambda}{2\lambda} \right]^{i-1} + \sigma_n^2 \\ &\quad + E\{[\Delta\alpha_{i-1}^f(k)]^2\}\sigma_x^2(1-\lambda)^2 \left[\frac{1+\lambda}{2\lambda} \right]^{i-1} \end{aligned} \quad (9.138)$$

$$E\{[\Delta c_i^f(k)]^2\} = \frac{2\lambda(1-\lambda^2)}{\sigma_x^2} \left[\frac{1+\lambda}{2\lambda} \right]^{i-1} E\{[\Delta\alpha_{i-1}^f(k)]^2\} + \sigma_n^2 \quad (9.139)$$

$$\begin{aligned} E\{[\Delta e_i^b(k)]^2\} &= \sigma_x^2 \left[\frac{2\lambda}{1+\lambda} \right]^{i-1} E\{[\Delta c_i^b(k)]^2\} + \lambda E\{[\Delta e_{i-1}^b(k)]^2\} \\ &\quad + E\{[\Delta s_i^b(k)]^2\}\sigma_x^2 \frac{\lambda}{1+\lambda} \left[\frac{2\lambda}{1+\lambda} \right]^{i-1} \\ &\quad + \lambda(1-\lambda)E\{[\Delta s_i^b(k)]^2\} + \sigma_n^2 \end{aligned} \quad (9.140)$$

The other two remaining values required to compute $E\{[\Delta e(k)]^2\}$ can be derived from step (S.12) and are shown below.

$$\begin{aligned}
 E\{[\Delta\beta_{i-1}(k)]^2\} &= \frac{\lambda}{1-\lambda^2} E\{[\Delta c_i^f(k)]^2\} E\{\beta_{i-1}^2(k)\} \\
 &+ \frac{1}{1+\lambda} E\{[\Delta e_{i-1}(k)]^2\} + E\{e_{i-1}^2(k)\} + \frac{\sigma_n^2}{1-\lambda^2} \\
 &+ \frac{1}{1-\lambda^2} E\{[\Delta s_i^f(k)]^2\} \tag{9.141}
 \end{aligned}$$

$$\begin{aligned}
 E\{[\Delta e_i(k)]^2\} &= \lambda E\{[\Delta e_{i-1}(k)]^2\} + E\{[\Delta c_i^f(k)]^2\} E\{e_{i-1}^2(k)\} \\
 &+ (1-\lambda)\lambda E\{[\Delta\beta_{i-1}(k)]^2\} \\
 &+ \lambda E\{[\Delta s_i^f(k)]^2\} E\{\beta_{i-1}^2(k)\} + \sigma_n^2 \tag{9.142}
 \end{aligned}$$

9.3.2.6 Mean squared value of $\Delta e(k)$

Using step (S.18), the mean squared accumulated quantization error of the *a posteriori* error signal is given by

$$E\{[\Delta e(k)]^2\} = \lambda^N E\{[\Delta e_{N+1}(k)]^2\} + E\{[\Delta\alpha_{N+1}(k)]^2\} \frac{\sigma_r^2}{\lambda^i} + \sigma_n^2. \tag{9.143}$$

9.3.3 Simulation results

Intensive simulations were performed to verify the accuracy of derived relations in both infinite and finite-precision. Different values of λ , σ_x^2 and different number of bits were used. In the simulations, 2s complement rounding was used, the input was white Gaussian noise with $\sigma_x^2 = -30$ dB, $\lambda = 0.99$, the measurement error signal had variance $\sigma_r^2 = -70$ dB, and an MA process of order 2 was used. A total of 10,000 points were calculated in both finite-precision and infinite-precision and the last 9000 samples were averaged. The results of simulated and calculated results for $E\{[\Delta e(k)]^2\}$ are displayed in Table 9.6.

Simulations with different values of λ were also performed. On these simulations, 15 bits were used. The input signals were the same as in the previous simulations. The results are shown in Table 9.7.

Table 9.6 Simulation results of $E\{[\Delta e(k)]^2\}$ – different number of bits ($\lambda = 0.99$).

Number of Bits	Simulated (dB)	Calculated (dB)
10	-60.66	-59.94
15	-89.55	-90.05
20	-119.46	-120.15
30	-178.84	-180.36

Table 9.7 Simulation results of $E\{\Delta e(k)^2\}$ – different values of λ (15 bits).

λ	Simulated (dB)	Calculated (dB)
0.90	-87.75	-88.96
0.95	-88.67	-89.67
0.98	-89.40	-89.98
0.99	-89.63	-90.05

9.4 Conclusion

This chapter describes propagation models for the error generated by quantization in two important QRD-RLS algorithms, namely the conventional and the FQRD-lattice algorithms. These algorithms are among the sub-class of algorithms that are known to have stable behavior in finite-precision implementations. The approach presented consists of deriving the steady-state mean squared values of all internal variables of the algorithms as well as the mean squared values of their errors originating from quantization.

As a rule, the analytical expressions for the internal variables allow access to estimates of their dynamic range, which in turn should be employed in determining their required wordlengths. In addition, the expressions related to the quantization effects provide tools to estimate the loss in accuracy originating from error propagation in the internal variables. The derived expressions are all verified to be quite accurate through the simulations presented.

References

1. K. J. R. Liu, S.-F. Hsieh, K. Yao, and C.-T. Chiu, Dynamic range, stability, and fault-tolerant capability of finite-precision RLS systolic array based on Givens rotations. *IEEE Transactions on Circuits and Systems*, vol. 38, no. 6, pp. 625–636 (June 1991)
2. S. Leung and S. Haykin, Stability of recursive QRD-LS algorithms using finite-precision systolic array implementation. *IEEE Transactions on Acoustics, Speech, and Signal Processing*, vol. 37, no. 5, pp. 760–763 (May 1989)
3. S. Haykin, *Adaptive Filter Theory*. Prentice-Hall, Englewood Cliffs, NJ, USA (1991)
4. J. G. McWhirter, Recursive least-squares minimization using a systolic array. *SPIE Real-Time Signal Processing VI*, vol. 431, pp. 105–112 (January 1983)
5. W. H. Gentleman and H. T. Kung, Matrix triangularization by systolic arrays. *SPIE Real-Time Signal Processing IV*, vol. 298, pp. 19–26 (January 1981)
6. P. S. R. Diniz and M. G. Siqueira, Finite precision analysis of the QR-recursive least squares algorithm. *IEEE Transactions on Circuits and Systems II: Analog and Digital Signal Processing*, vol. 42, pp. 334–348 (May 1995)
7. A. Papoulis, *Probability, Random Variables, and Stochastic Processes*. McGraw-Hill Book Company, New York, NY, USA (1965)
8. C. Caraiscos and B. Liu, A roundoff error analysis of the LMS adaptive algorithm. *IEEE Transactions on Acoustics, Speech and Signal Processing*, vol. ASSP-32, no. 1, pp. 34–41 (February 1984)

9. C. G. Samson and V. U. Reddy, Fixed point error analysis of the normalized ladder algorithm. *IEEE Transactions on Audio, Speech, and Signal Processing*, vol. ASSP-31, no. 5, pp. 1177–1191 (October 1983)
10. N. Kalouptsidis and S. Theodoridis, *Adaptive System Identification and Signal Processing Algorithms*, Prentice-Hall, Upper Saddle River, NJ, USA (1993)
11. M. G. Siqueira and P. S. R. Diniz, Infinite precision analysis of the QR-recursive least squares algorithm. *IEEE International Symposium on Circuit and Systems, ISCAS'93*, Chicago, USA, pp. 878–881 (May 1993)
12. M. G. Siqueira, P. S. R. Diniz, and A. Alwan, Infinite precision analysis of the fast QR decomposition RLS algorithm. *IEEE International Symposium on Circuits and Systems, ISCAS'94*, London, UK, vol. 2, pp. 293–296 (May–June 1994)